

Supplemental Material of "An Iterative Linear Method with Variable Shear Stress Magnitudes for Estimating the Stress Tensor from Earthquake Focal Mechanism Data: Method and Examples"

Eric Beaucé^{1,3}, Robert D. van der Hilst¹, and Michel Campillo^{2,1}

¹Department of Earth, Atmospheric, and Planetary Sciences, Massachusetts Institute of Technology, Cambridge, MA, United States

²Institut des Sciences de la Terre, Université Grenoble Alpes, Grenoble, France

³Lamont-Doherty Earth Observatory, Columbia University, NY, United States

Description of the Content

Figures S1 to S7.

Content

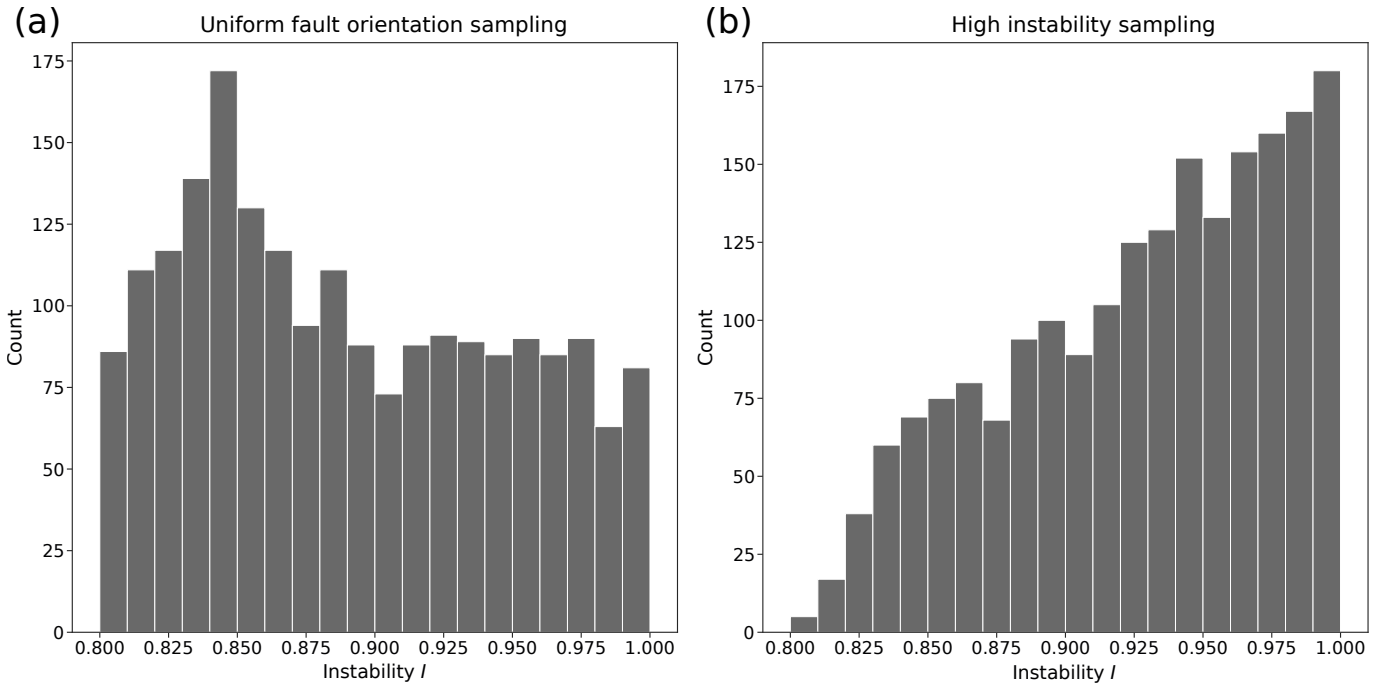


Figure S1: Distribution of fault instabilities for (a): the uniform fault orientation sampling, and (b): the high instability preferential sampling.

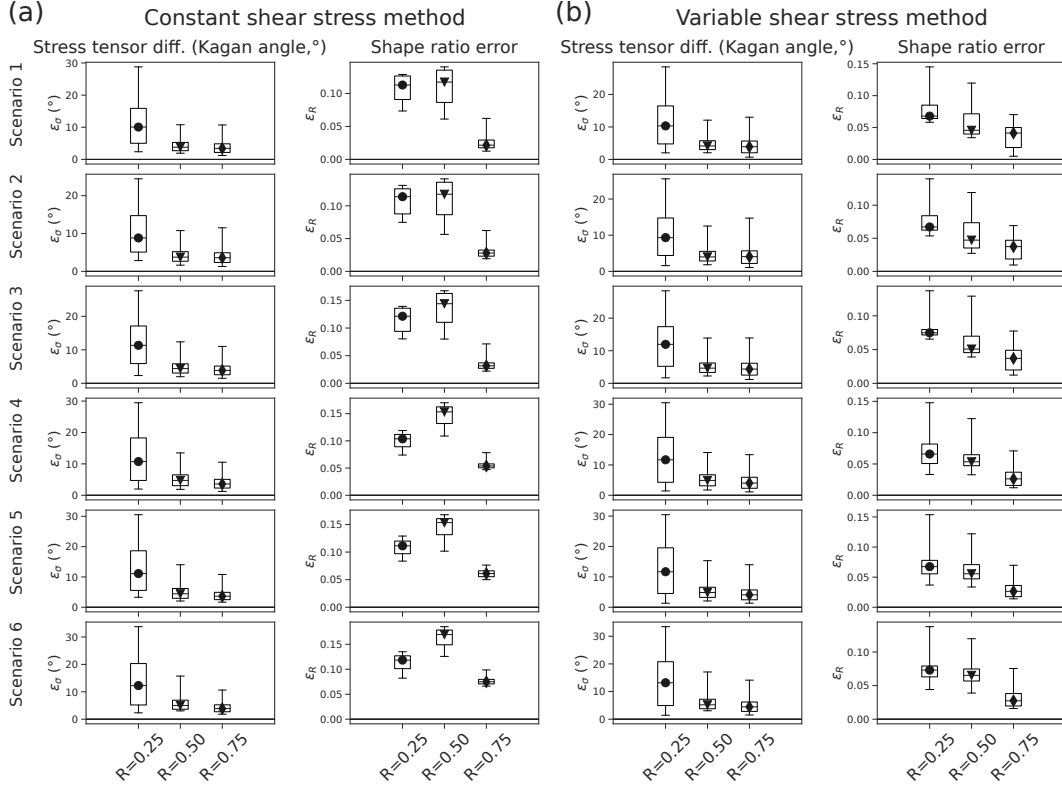


Figure S2: Summary of the errors of **(a)**: the constant shear method and **(b)**: the variable shear method. Each column shows the distribution of one error parameter (ϵ_σ and ϵ_R), represented by a box plot. Each row shows the results for a different data scenario (see Table 1 in the main manuscript). The box plots show the results for the three shape ratio values (filled dots: $R = 0.25$, inverted triangles: $R = 0.50$; diamonds: $R = 0.75$). Symbols indicate the median, limits of the boxes are the first and third quartiles, and whiskers are the 2.5 and 97.5 percentiles (*i.e.* the boxplots cover the 95% confidence interval).

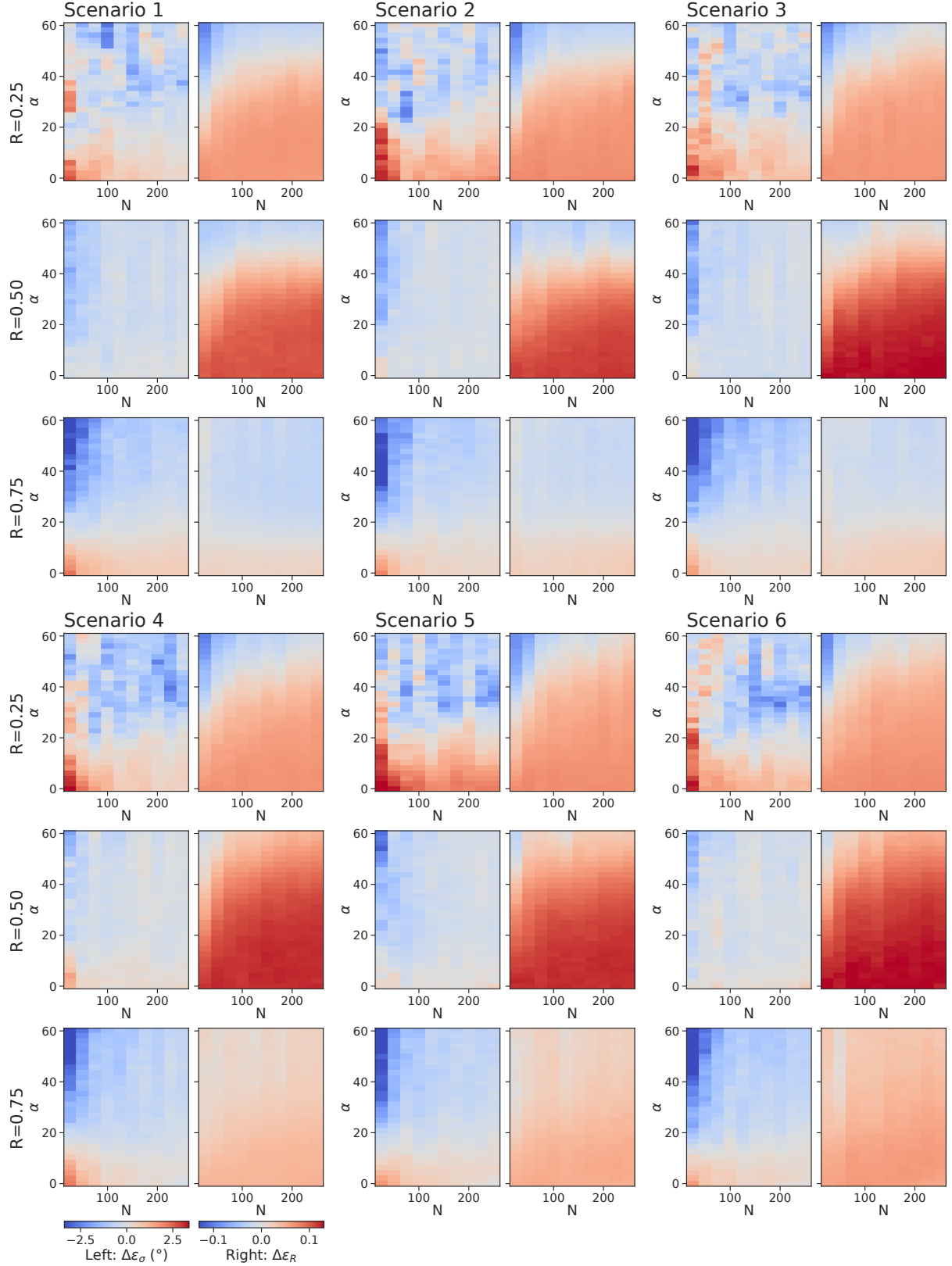


Figure S3: Error differences between the constant and the variable shear stress methods for every data scenario. The figure reads as a table where each 2-panel subfigure corresponds to a data scenario (column) and a shape ratio (row). See Table 1 in the main manuscript for the definitions of the data scenarios. Inside each subfigure, the left panel shows the error difference in stress orientations and the right panel shows the error difference in shape ratios, as a function of data set size (x-axis) and noise level (y-axis).

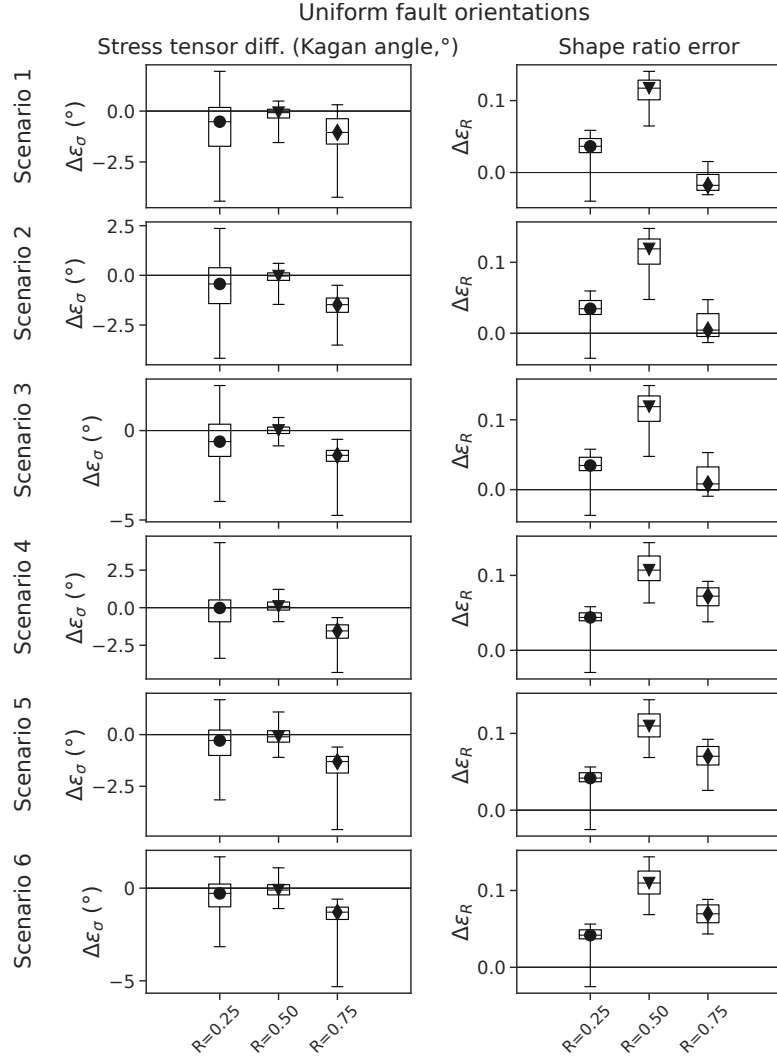


Figure S4: Summary of the error differences between the constant shear and variable shear methods with the uniform fault orientation sampling strategy (see Figure 2 in the main text). Each of the two columns shows the distribution of one relative error parameter ($\Delta\epsilon_\sigma$, $\Delta\epsilon_R$). Same legend as Figures S2.

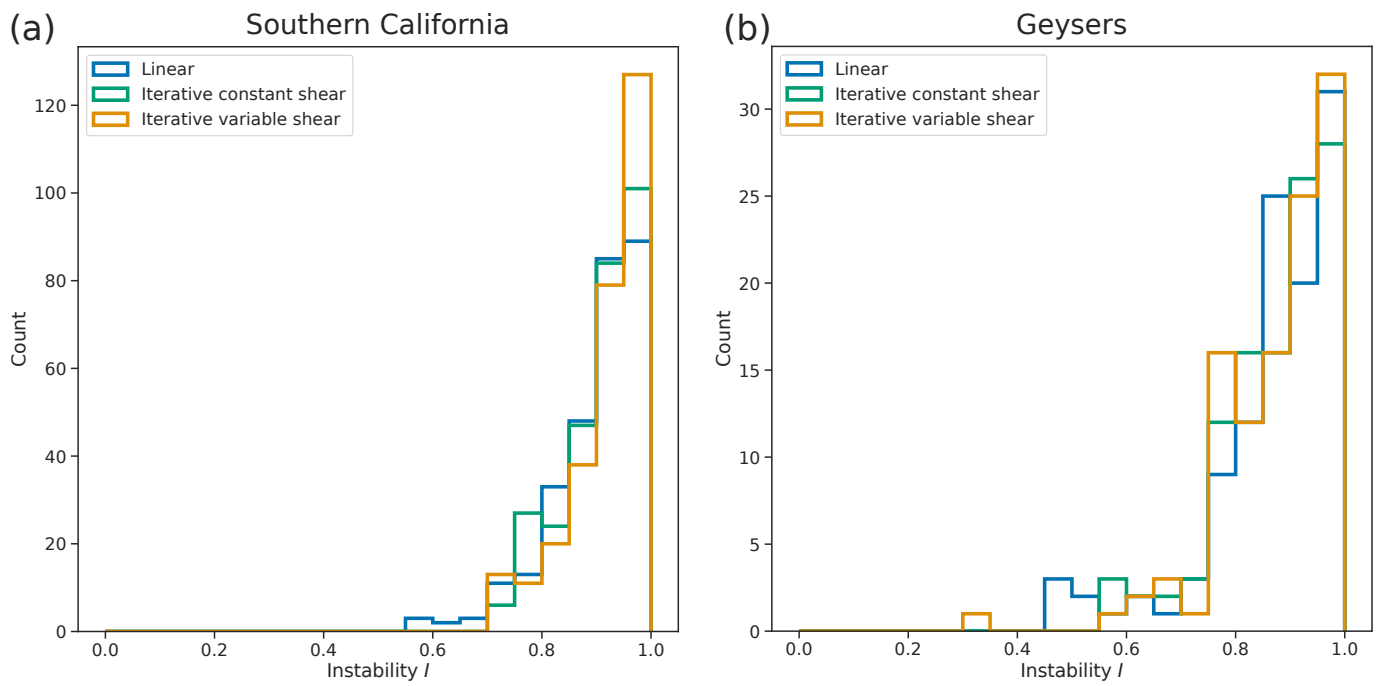


Figure S5: Instabilities estimated from the inverted stress tensors on **(a)**: The Southern California data set, and **(b)**: The Geysers data set.